**AIP Conference Proceedings**

# Numerical investigation of heat transfer and pressure loss of flow through a heated plate mounted by perforated concave rectangular winglet vortex generators in a channel

Syaiful, Nakula Kusuma,  Muchammad, Retno Wulandari, Nazarudin Sinaga, Ahmad Siswantara, and Myung-Whan Bae

View Online   Export Citation

## ARTICLES YOU MAY BE INTERESTED IN

Rheological characteristics of non-Newtonian mud slurry flow using spiral pipes
AIP Conference Proceedings **2227**, 020001 (2020); https://doi.org/10.1063/5.0001003

Module development of piping system design with rule based algorithms
AIP Conference Proceedings **2227**, 020019 (2020); https://doi.org/10.1063/5.0001000

Review of electric power steering type column steering with booster motor and future research for EV-Bus
AIP Conference Proceedings **2227**, 020016 (2020); https://doi.org/10.1063/5.0000945

AIP
Publishing

# Numerical Investigation of Heat Transfer and Pressure Loss of Flow Through a Heated Plate Mounted by Perforated Concave Rectangular Winglet Vortex Generators In a Channel

Syaiful[1, a], Nakula Kusuma[1], Muchammad[1], Retno Wulandari[2], Nazarudin Sinaga[1], Ahmad Siswantara[3], Myung-Whan Bae[4]

[1]*Universitas Diponegoro, Semarang, Jawa Tengah, Indonesia*
[2]*Universitas Negeri Malang, Jawa Timur, Indonesia*
[3]*Univesitas Indonesia*
[4]*Gyeongsang National University, Republic of Korea*

[a]Corresponding author : syaiful.undip2011@gmail.com

**Abstract.** The low thermal conductivity of air in fin-and-tube heat exchangers causes high thermal resistance of the air side and results in a low heat transfer rate. This heat transfer rate on the air side can be improved by increasing the heat transfer coefficient. One way to increase the heat transfer coefficient on the air side is to use a vortex generator (VG), which can generate longitudinal vortex (LV) increasing fluid mixing. Therefore, this study aims to numerically analyze heat transfer characteristics and pressure drop of airflow through a heated plate by installing VG in a rectangular channel. Vortex generators (VGs) used in numerical modeling are rectangular winglet pairs (RWPs) and concave rectangular winglet pairs (CRWPs) with 30° attack angle. The number of pairs of VG is varied by one, two, and three with/without holes. The velocity of airflow varies in the range of 0.4-2.0 m/s at intervals of 0.2 m/s. The simulation results show that in the configuration of the three pairs of VG, the decrease in the convection heat transfer coefficient in the case of the perforated CRWP is 3.98% of the CRWP without holes at a velocity of 2.0 m/s. While in the configuration of three pairs of perforated RWP VGs, the decrease in convection heat transfer coefficient is 5.87% from RWP without holes at a velocity of 2.0 m/s. In the configuration of three pairs of perforated VGs at the highest velocity, the decrease in pressure drop in the CRWP and RWP cases is 30.73% and 13.87% of the VGs without holes, respectively.

**Keywords**: Heat transfer; Pressure loss; Perforated concave rectangular winglet; Longitudinal vortex intensity; Field synergy principle

## INTRODUCTION

Compact heat exchangers (CHXs) are widely used in the chemical industry, petroleum industry, automotive industry, refrigeration industry, and others. Fin-and-tube is one type of compact heat exchanger that is widely used, especially in household cooling (Awais and Arafat, 2018). The low thermal conductivity of the air causes a high thermal resistance on the air side and results in a low heat transfer rate (Zhan et al., 2018). This heat transfer rate on the air side can be improved by increasing the heat transfer coefficient (Zeeshan et al., 2018).

Increasing the rate of heat transfer can be done by three methods, namely active, passive, and combined. The difference between active and passive methods is in external power (Han et al., 2018). Active methods such as fluid vibrations, surface vibrations, electroscopic fields, and suction layer boundaries require external power to increase the heat transfer rate, while the passive method does not use the external power to increase the heat transfer rate (Awais and Arafat, 2018). Thepassive method by extending the surface and coating the surface is more cost effective and easy to use compared to the active method. Therefore, increasing the heat transfer rate with the passive method is more widely used in research (Liu et al., 2018).

Vortex generator (VG) is one of the passive methods that has been widely used to increase heat transfer rates in heat exchangers (Han et al., 2018). VG is widely applied to fin-and-tube heat exchangers to increase the heat transfer rate on the air side by generating longitudinal vortex (Lu & Zhai, 2019).

Various studies have been conducted relating to VG to increase the heat transfer coefficient. Hung Yi Li et al. (2017) conducted experimental and numerical research on pin fin heat sink using delta winglet vortex generator.

Their results show that an increase in Reynolds number decreases thermal resistance. The highest heat transfer rate is observed for VG, which is installed in the center of the heat sink on both sides. In addit ion, an increase in heat transfer rate is also influenced by the addition of VG height. However, the increase in height from VG increases pressure drop. Meanwhile, Mohammad Oneissi et al. (2018) conducted a numerical study on parallel plate fin heat exchanger installed by delta winglet (DWP) type and inclined projected winglet pair (IPWP) with rib configuration, which IPWP is a new type of VG configuration. Their results show that the IPWP-M configuration provides an increase in the heat transfer rate of 7.1% higher than DWP and 2.3% greater than the IPWP.

Geofeng Lu et al. (2018) conducted a numerical study on the fin and oval tube heat exchanger with teardrop delta vortex generators mounted with a common flow-up configuration. Their simulation results prove that teardrop delta VG is better at increasing heat transfer rates and decreasing flow resistance. Also, Y. Xu (2018) conducted an experimental study on a circular tube mounted with VG type winglet delta with variations in attack angle ($\beta$) of $0^o$, $15^o$, $30^o$, and $45^o$, variations in block ratios (B) of 0.1, 0. 2, and 0.3, differences in row values (N) of 4, 8, and 12, and relative pitch ratio variations of 4.8, 2.4, and 1.6. The results of their research revealed that the Nusselt number decreases with increasing pitch ratio, however the Nusselt number increases with increasing Reynolds number, attack angle, and blockage ratio.

Hui Han et al. (2019) investigated numerically fin and tube heat exchangers mounted by VG type  equal perimeter arc winglet, curved equal area arc winglet, and curved equal perimeter arc winglet. They found that Nusselt numbers in the case of equal perimeter arc VGs fin, curved equal area arc VGs fin, and curved equal perimeter arc fin VGs are increased by 11.5%, 19.9%, and 35.9% from rectangular winglet vortex generator, respectively. Then, in the case of the curved equal perimeter arc VGs fin, the Nusselt number and pressure drop increase by 22.2% and 13.5% respectively from the equal perimeter arc VGs fin.

Syaiful et al. (2017) investigated numerically on rectangular channels mounted concave delta winglet (CDWP) VG with $30^o$ attack angle and variation in the number of pairs of VGs. The results of their study showed that the CDWP VG gave an increase in heat transfer rate and a pressure drop greater than DWP VG. Syaiful et al. (2018) have also studied the improvement of heat transfer in fin and tube heat exchanger by installing concave rectangular winglets. They found that the installation of CRWP at Re = 364 increased the convection heat transfer coefficient and pressure drop by 102% and 216.8% from baseline, respectively. Based on the results of previous studies, it can be concluded that the addition of VGs can increase the heat transfer rate. However, the use of VGs also has an impact on the increase in pressure drop. Therefore, the current study considers the use of VGs with a lower pressure drop while maintaining a high heat transfer rate. The use of perforated CRWP VGs has never been done in previous studies.

# PHYSICAL MODEL
## Experimental set up

Experiment on the effect of VG on the heat transfer rate and pressure drop was carried out on rectangular channel with length, height, and width of 370 cm, 18 cm and 8 cm, respectively in which walls were made of glass with a thickness of 1 cm as shown in Figure 1. A blower was placed at one end to suck air into the channel. The air flow velocity inside the channel was regulated using an inverter (Mitsubishi Electric type FR-D700 with an accuracy of ± 0.01) and varied in the range of 0.4 m/s to 2.0 m/s with intervals of 0.2 m/s. In this study, the air was passed through a straightener with a length of 290 mm to obtain a uniform flow distribution. VGs were mounted on a heated plate 1 mm thick, 500 mm long, and 155 mm wide. The number of pairs of VG and with/without holes was varied from one to three pairs. A hot wire anemometer (Lutron type AM-4204 with accuracy ± 0.1) was placed 27 cm behind the straightener to measure the air velocity inside a channel. In

thermal performance testing, the test specimen was heated at a constant heat rate of 35 W using a regulator heater connected to a wattmeter (Lutron DW- 6060 with an accuracy of ± 1.0) to monitor the heat rate induced into the plate. Type K thermocouples were used to measure inlet air, outlet air, and test specimen wall that was associated with data acquisition (Advantech type USB- 4718 with accuracy ± 0.001), in which data acquisition was connected to the CPU so that temperatures can be monitored and stored. In pressure drop testing, two pitot tubes were connected with a pressure micromanometer (Fluke type 922 with accuracy ± 0.05) to monitor the pressure difference between inlet and outlet of the test specimen.

## Numerical Model

Modeling was carried out on a rectangular channel that has been mounted by concave rectangular winglet pair (CRWP) and rectangular winglet pair (RWP) VGs. VGs were arranged using a common flow-down configuration with an attack angle (α) of 30° and a longitudinal pitch distance of 125 mm. The number of pairs of VG with/without holes was varied from one, two, and three pairs. VG with three holes has a diameter of (d) 5 mm each. The geometry of CRWP and RWP VGs with/without holes is shown in Figure 2. Geometric parameters in both types of VG can be seen in Table 1. Figure 3 shows the top view of RWP and CRWP VGs. The first row (P) distance with the inlet channel is 125 mm, while the transverse leading edge between winglet pairs VG (S) is 20 mm.
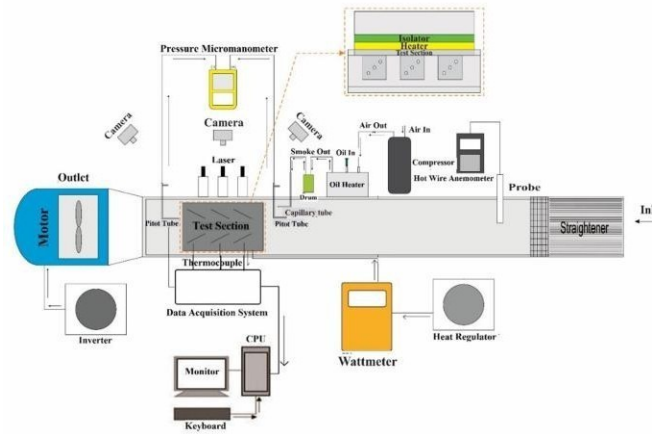


**Figure 1**. Experimental set-up

The computational domain, as shown in Figure 4, consists of the inlet extended region and the outlet extended region. The size of the computational domain in this simulation is 18,500 mm length (L), 75.5 mm width (W), and 65 mm height (H). The function of the inlet extended region is to ensure the air flow in the inlet of the test plate in the channel is a fully developed flow, while the outlet extended region functions to prevent the reverse flow of air on the channel.

**Table 1**. Geometric parameters of vortex generators

| VGs | α(°) | a(mm) | cv(mm) | dv(mm) | ev(mm) | ch(mm) | dh(mm) | eh(mm) | t (mm) | R(mm) |
|---|---|---|---|---|---|---|---|---|---|---|
| CRWP without holes | 30 | 59 | - | - | - | - | - | - | 40 | 58 |
| CRWP with holes | 30 | 59 | 29.56 | 44.56 | 14.56 | 20 | 30.15 | 9.85 | 40 | 58 |
| RWP without holes | 30 | 60 | - | - | - | - | - | - | 40 | - |
| RWP with holes | 30 | 60 | 30 | 45 | 15 | 20 | 30 | 10 | 40 | - |

In this numerical simulation, the flow is assumed to be steady, incompressible, and the physical properties of the fluid are constant. Viscous dissipation and body force are ignored. The Reynolds number determined

from the flow velocity in the range 0.4-2 m/s with an interval of 0.2 m/s is 1600 <Re <9000. Based on these assumptions, the governing equations used to solve this problem are the mass, momentum and energy conservations. In this numerical simulation, the standard $k$-$\omega$ model was used to model turbulent flow.
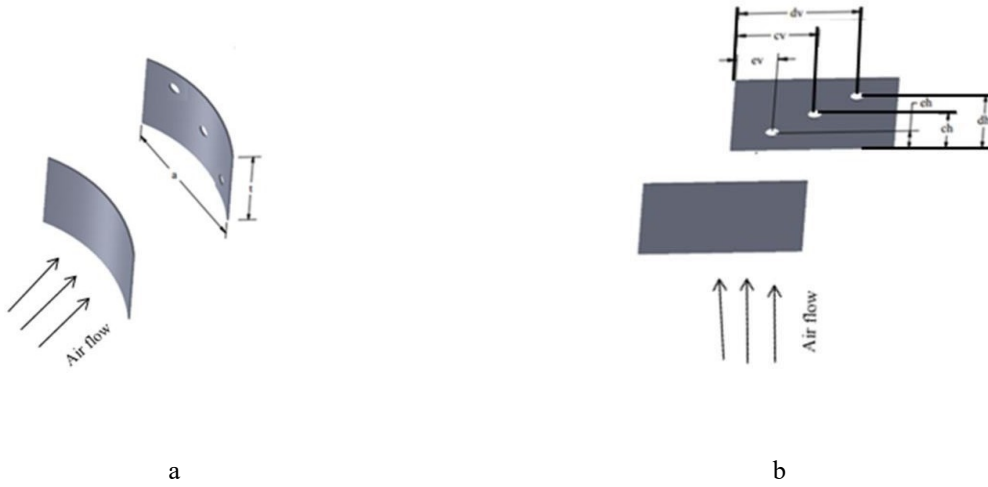


a          b

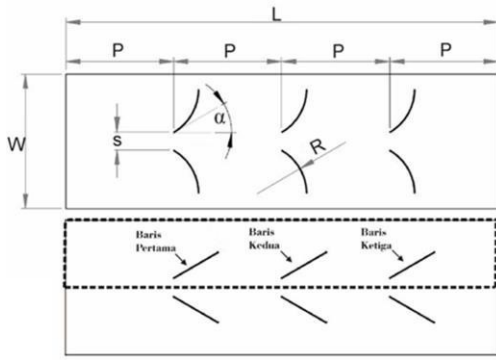**Figure 2**. Vortex generator with/without holes: a) CRWP, b) RWP
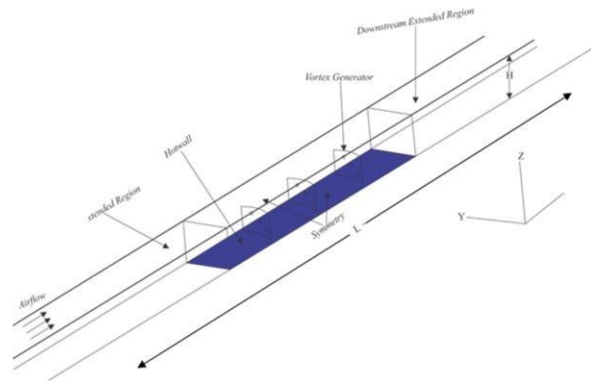


**Figure 3.** Top view of CRWP and RWP VGs       **Figure 4**. Domain computation

Boundary conditions are needed to solve governing equations that are applied in this study. The flow velocity in the inlet was determined uniformly in the direction of flow, while the components of the velocity across the flow (y and z directions) were set to zero. The temperature in the inlet was determined the same as the outside air temperature. The outlet boundary condition was chosen away from the flow geometry disturbance and reaches a fully developed. This indicates that the gradient of all variables in the direction of flow except the pressure is zero. The boundary conditions on the upper wall of the plate mounted by VGs were set no slip and adiabatic. The no- slip boundary condition was also applied to a hot wall with a constant temperature. Symmetry boundary conditions were determined with no flow across this boundary.

To obtain good results on the velocity, temperature, and pressure values in this simulation, precision in the meshing process is required. The hexahedral mesh was used in the upstream and downstream extended regions because of its simple geometry. The tetrahedral mesh type was used for areas close to VG because the geometry is more complex in the presence of VG. The use of tetrahedral mesh is intended to get more accurate results in the area so that it can show the separation of flow and secondary flow on the channel.

An independent grid test was carried out to ensure that the numerical simulation results are not affected by the number of grids. In this independent grid test, simulations were carried out on the computational domain of three pairs of CRW VGs with four variations in the number of grids, namely 1,262,840,

1,478,060, 1,661,610 and 1,868,587 at a flow velocity of 0.4 m/s. From the test of the four grid variations, the number of grids where the smallest change of the convection heat transfer coefficient was found on the grid with the number of elements of 1,661,610. Therefore, the number of elements used in this numerical modeling was 1,660,610.

In this simulation, the finite volume method (FVM) was used in commercial CFD software to analyze the characteristics of thermo-hydraulic flow through a heated plate installed by VG. Laminar flow was modeled using a laminar model, while the turbulent flow was modeled with k-ω because this model is suitable for modeling fluid flow in the viscous region (An & Fung, 2018). The SIMPLE model was adopted as a procedure for calculating the pressure in continuity and momentum equations. Momentum, turbulent kinetic energy, specific dissipation rate, and energy equations were discretized using second-order upwind schemes. The convergence criterion specified in the continuity, momentum, and energy equations was $10^{-5}$, $10^{-5}$, $10^{-8}$, respectively.

# RESULTS AND DISCUSSION
## Longitudinal Vortex Intensity

In this study, a dimensionless number in KeWei Song's research et al. (2019) was used to represent the longitudinal vortex strength. Figure 5 shows a comparison of the local longitudinal vortex intensity for the case of RWP and CRWP VGs at a velocity of 2 m/s. From Figure 5, it is found that the longitudinal intensity of vortex in the CRWP case is observed to be higher than that of RWP because the frontal area of the CRWP VGs is greater than that of RWP (Guo et al., 2005). There is instability in the centrifugal force when the flow passes the CRWP VGs (Syaiful et al., 2017) and the large pressure difference between VGs on the downstream and upstream sides (Qian et al., 2018). The longitudinal vortex intensity in cases of CRWP and RWP tends to decrease with increasing distance from VGs in the downstream region due to viscous dissipation (Lu and Zhou, 2016). Holes in RWP and CRWP VGs result in the formation of a jet flow that interferes with the formation of a longitudinal vortex (Han et al., 2018) so that the longitudinal vortex intensity is lower than without holes. In CRWP VGs, the highest decrease in longitudinal vortex intensity for the case of three pairs with holes is 18.79% of those without holes at location x/L = 0.52.
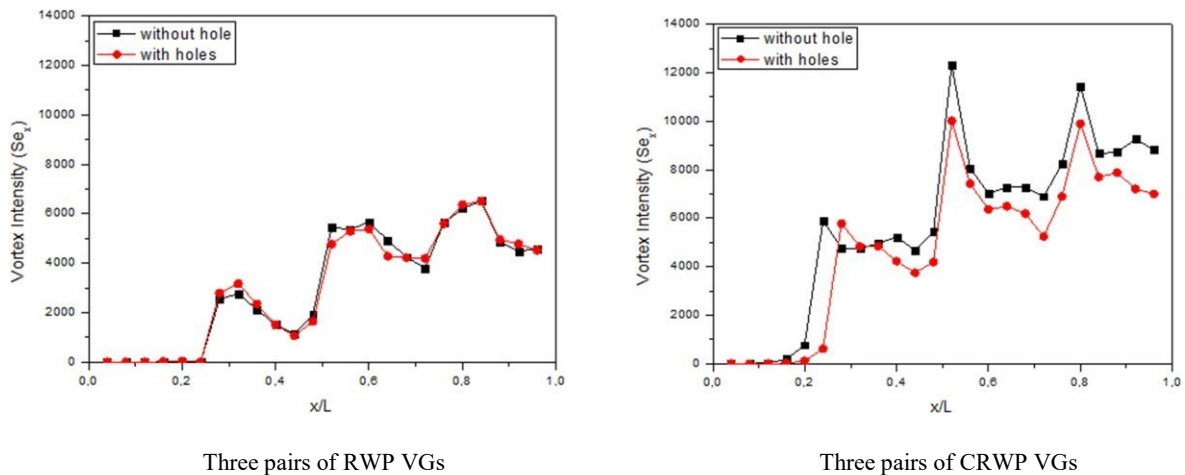


Three pairs of RWP VGs         Three pairs of CRWP VGs
**Figure 5**. Longitudinal vortex intensity at a velocity of 2 m/s

## Effect of Longitudinal Vortex on Average Convection Heat Transfer Coefficient

Figures 6 and 7 show a comparison of the average convection heat transfer coefficients in the RWP and CRWP cases for experiment and calculation results. Overall, the convection heat transfer coefficient increases with increasing Reynolds number. From Figures 6 and 7, it is found that the use of CRWP VGs increases the convection heat transfer coefficient higher than that of RWP because CRWP generates

longitudinal vortex stronger than those from RWP at the same flow velocity (Syaiful et al., 2018). In RWP and CRWP, increasing convection heat transfer coefficients with three pairs configuration with perforated VGs at the highest Reynolds numbers are 37.59% and 46.44% from the baseline, respectively.
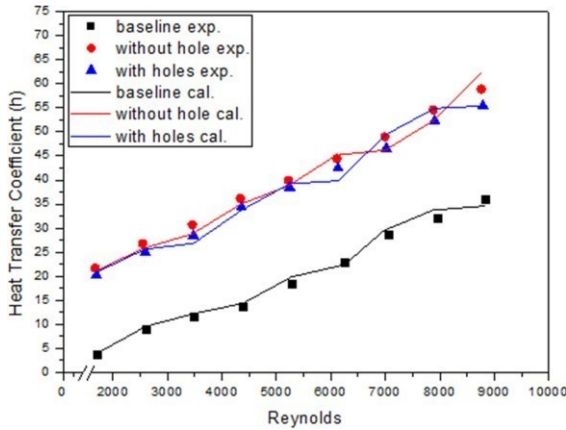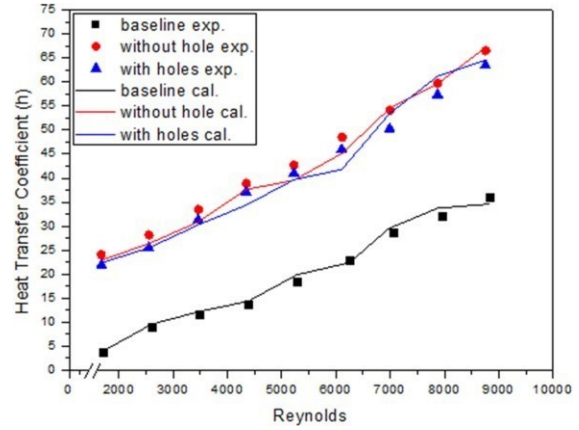


**Figure 6**. Comparison between experiment and simulation results of convection heat transfer coefficient with variations in Reynolds numbers for installation of RWP VG with and without holes



**Figure 7**. Comparison between experiment and simulation results of convection heat transfer coefficient with variations in Reynolds numbers for installation of CRWP VG with and without holes

## Effect of Longitudinal Vortex on Pressure Drop

Figures 8 and 9 show a comparison of the pressure drop values between the experimental results and simulations on the installation of RWP VGs and CRWP with variations in Reynolds numbers. From the two figures, it can be stated that the pressure drop of the simulation and experimental results increase with increasing Reynolds numbers for all cases. In general, the installation of RWP and CRWP VGs in the channel resulted in the formation of a vortex which caused a deviant flow from the main flow to yield in an increase in pressure drop (Keiwei Song et al., 2019). The pressure drop produced in the CRWP case is higher than that of the RWP case because the growth of boundary layer and fluid mixing for CRWP VGs is more disruptive than that of RWP (Hemant Naik et al., 2018) and the projection size of the flow contact area in the CRWP is greater than that of RWP (Syaiful et al., 2018). The increase in pressure drop for RWP cases with holes at the highest Reynolds number reaches five times than the baseline case. By using CRWP VGs, the pressure drop value can reach 18 times higher than that from the baseline at the highest Reynolds number. Holes in RWP VGs and CRWP cause a decrease in the pressure drop value due to jet flow, which makes the backflow area at low velocities smaller than those without holes (Zhimin Han et al., 2018). By installing CRWP VGs with holes, the pressure drop value can be reduced to 30.7% of those without holes.
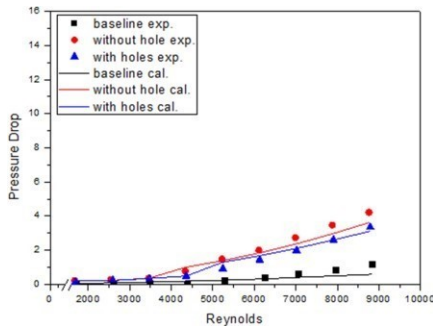


**Figure 8**. Comparison between experiment and simulation results of pressure drop with variations in Reynolds numbers for installation of RWP VG with and without holes
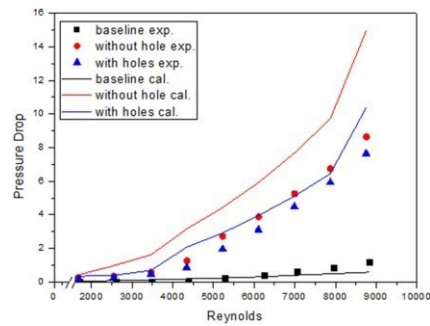


**Figure 9**. Comparison between experiment and simulation results of pressure drop with variations in Reynolds numbers for installation of CRWP VG with and without holes

## Heat transfer analysis using field synergy principle

Guo et al. (2005) studied increasing heat transfer rates using the field synergy principle (FSP) method. Increasing the heat transfer rate can be identified by decreasing the intersection angle between the velocity vector with a temperature gradient. Figure 12 shows the local field synergy angle for the RWP and CRWP cases at a velocity of 2.0 m/s. From Figure 12, it is shown that the installation of CRWP VGs results in a decrease in synergy angle more considerable than that of RWP because the strength of longitudinal vortex generated by the CRWP is higher than that of RWP (Syaiful et al., 2018; Lu and Zhou, 2016). In the case of CRWP with the same configuration and flow velocity, the minimum peaks are 76.47°, 76.59°, and 78.22° for x/L = 0.32, 0.56, and 0.8, respectively. Holes in VGs cause an increase in synergy angle due to a decrease in convection heat transfer coefficient (Guo et al., 2005).
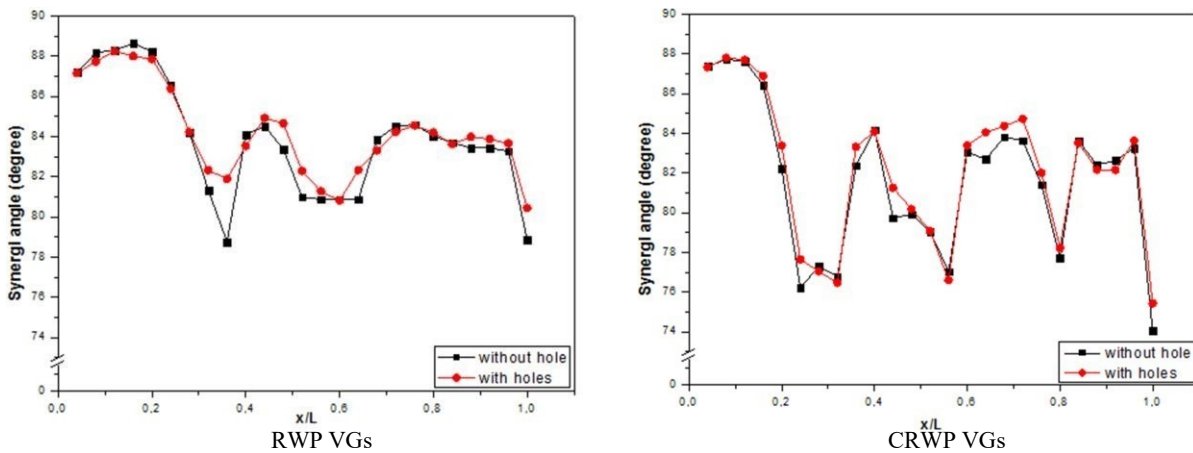


**Figure 10.** Comparison of local field synergy angle between RWP and CRWP VGs cases at velocity of 2 m/s

## CONCLUSION

From the results of simulations and experiments, it was found that the installation of perforated VGs decreases the convection heat transfer coefficient and pressure drop. Reducing convection heat transfer coefficients for the case of three pairs of perforated RWP and CRWP VGs at the highest Reynolds number is 5.87% and 3.98%, respectively, compared to those without holes. The decrease in pressure drop at highest Reynolds number for perforated RWP and CRWPs VGs reached 13.86% and 30.73%, respectively, from those without holes. Holes in VGs caused an increase in synergy angel. The increase in average synergy angle for three pairs perforated RWP, and CRWP VGs at a velocity of 2.0 m/s was $0.44^o$ and $0.33^o$ for those without holes.

## ACKNOWLEDGEMENT

# REFERENCES

1. Feilong Zhan, Dawei Zhuang, Guoliang Ding, Peiling Ju, (2018), Influence of wet-particle deposition on air- side heat transfer and pressure drop of fin-and-tube heat exchangers, International Journal of Heat and Mass Transfer, Volume 124, pp. 1230–1240.

2. Hemant Naik, S. Harikrishnan, Shaligram Tiwari, (2018), Numerical investigations on heat transfer characteristics of curved rectangular winglet placed in a channel, International Journal of Thermal Sciences, Volume 129, pp. 489–503.

3. Huan-ling Liu, Heng Li, Ya-ling He, Zeng-tao Chen, (2018), Heat transfer and flow characteristics in a circular tube fitted with rectangular winglet vortex generators, International Journal of Heat and Mass Transfer, Volume 126, pp. 989–1006.

4. Hui Han, Shaowei Wang, Li Sun, Yuxing Li, Shuo Wang, (2019), Numerical study of thermal and flow characteristics for a fin-and-tube heat exchanger with arc winglet type vortex generators, International Journal of Refrigeration, Volume 98, pp. 61–69.

5. Hung-Yi Li, Wan-Rong Liao, Tian-Yang Li, Yan-Zuo Chang, (2017), Application of vortex generators to heat transfer enhancement of a pin-fin heat sink, International Journal of Heat and Mass Transfer, Volume 112, pp. 940–949.

6. KeWei Song, Toshio Tagawa, ZhongHao Chen, Qiang Zhang, (2019), Heat transfer characteristics of concave and convex curved vortex generators in the channel of plate heat exchanger under laminar flow, International Journal of Thermal Sciences, Volume 137, pp. 215–228.

7. Mohammad Oneissi, Charbel Habchid, Serge Russeila, Thierry Lemenand, Daniel Bougeard, (2018), Heat transfer enhancement of inclined projected winglet pair vortex generators with protrusions, International Journal of Thermal Sciences, Volume 134, pp. 541–551.

8. Mohd Zeeshan, Sujit Nath, Dipankar Bhanja, Aabir Das, (2018), Numerical investigation for the optimal placements of rectangular vortex generators for improved thermal performance of fin-and-tube heat exchangers, Applied Thermal Engineering, Volume 136, pp. 589–601.

9. Muhammad Awais, Arafat A., (2018), Heat and mass transfer for compact heat exchanger (CHXs) design: A state-of-the-art review, International Journal of Heat and Mass Transfer, Volume 127, pp. 359–380.

10. Syaiful, Astrid Ayutasari, Maria F. Soetanto, Ahmad Indra Siswantara, Myung-whan Bae, (2017), Thermo- hydrodynamics performance analysis of fluid flow through concave delta winglet vortex generators by numerical simulation, International Journal of Technology, Volume 7, pp. 1276-1285.

11. Syaiful, Imam Syarifudin, Maria F. Soetanto, Myung-whan Bae, (2018), Numerical simulation of heat transfer augmentation in fin-and-tube heat exchanger with various number of rows of concave rectangular winglet vortex generator. In: MATEC Web of Conferences, Volume 159, 02012.

12. Xu, M.D. Islam, N. Kharoua, (2018), Experimental study of thermal performance and flow behaviour with winglet vortex generators in a circular tube, Applied Thermal Engineering, Volume 135, pp. 257–268.

13. Zhimin Han, Zhiming Xu, Jingtao Wang, (2018), Numerical simulation on heat transfer characteristics of rectangular vortex generators with a hole, International Journal of Heat and Mass Transfer, Volume 126, pp. 993–1001.

14. Y. Guo, W.Q. Tao, R.K. Shah, (2005), The field synergy (coordination) principle and its applications in enhancing single phase convective heat transfer, International Journal of Heat and Mass Transfer, Volume 48, pp. 1797–1807.